Dimensional Dependence of Scaling Prefactors in Jamming

James D Sartor, Eric I Corwin
Department of Physics and Materials Science Institute,
University of Oregon, Eugene, Oregon 97403, USA

Sean A. Ridout
Department of Physics and Astronomy, University of Pennsylvania, Philadelphia, PA 19104, USA

(Dated: May 15, 2020)

No known analytic framework precisely explains all the phenomena observed in jamming. The replica theory for glass and jamming is a mean field theory which attempts to do so by working in the limit of infinite dimensions, such that correlations between neighbors are negligible. As such, results from mean field theory are not guaranteed to be observed in finite dimensions. However, many results in mean field for jamming have been shown to be exact or nearly exact in low dimensions. This suggests that the infinite dimensional limit is not necessary to obtain these results. In this paper, we perform precision measurements of two jamming scaling relationships from dimensions 2-10 in order to extract the prefactors to these scalings. While these prefactors should be highly sensitive to finite dimensional corrections to the mean field, we find the mean field predictions for these prefactors to be exact in low dimensions. This suggests that the mean field approximation is not necessary for deriving these prefactors, and as such, we present a first principles derivation for one, leaving the other as an open question.

Introduction – Granular materials exhibit universal properties regardless of the material properties of the individual grains [1–3]. Such properties are empirically found to depend on the distance to the jamming transition, characterized variously by pressure, packing fraction, or number of excess contacts, among others. Scaling theory summarizes and condenses the power law relationships found between such quantities, but no first principles theory of jammed systems at finite dimensions exists. The replica mean field theory of glasses and jamming has been shown to be exact in the infinite dimensional limit [4, 5]. To do so it relies on the assumption that there are no correlations between neighbors, fundamentally at odds with low dimensional systems. Despite the fact that low dimensional systems have highly correlated neighbors the scaling relations are precisely the same as those found in infinite dimensions [6–8]. Many other results predicted by the mean field have also been observed in low dimensional jamming, suggesting that they may be provable without the mean field approximation [2, 3, 9–12].

Here, we move one step further in the comparison between low dimensional jamming and mean field jamming by probing not only scaling relations but also prefactors between a handful of properties: pressure P, excess contacts δz, and excess packing fraction above jamming $\Delta\varphi$. We demonstrate the continued success of the mean field in describing low dimensional systems by quantitatively verifying the mean field predictions for these prefactors. Thus, the mean field approximation is overzealous: one need not have vanishing correlations in order to obtain these results. In this spirit we provide a first principles proof of the relation between pressure and excess packing fraction free of the mean field assumptions. These results call out for proofs for all of the other universal relations of the jamming transition.

Background – Granular materials undergo a jamming transition at a critical packing fraction φ_j. In a packing of N particles in d dimensions, the number of force bearing contacts between grains jumps abruptly from zero to $Z_c \approx Nd$, the minimum number sufficient to support global rigidity and thus global pressure [1]. The value of φ_j has been predicted by mean field theory to follow the asymptotic scaling [4, 13, 14]:

$$\varphi_j = \hat{C}_\varphi \frac{d \log d}{2^d} \tag{1}$$

with unknown prefactor $\hat{C}_\varphi$ that does not depend on dimension. While many scalings and behaviors from the mean field have been observed at low dimensions, measured values of φ_j differ considerably from this asympotic prediction. Here, we conjecture that perhaps φ_j is the *only* property in substantial disagreement with the mean field. As such we will express relations in terms of φ_j when possible and use measured values of φ_j rather than the asympotic form.

We limit our study to spherical particles interacting through a harmonic contact potential given by

$$U(\mathbf{r}_{ij}) = \varepsilon \left(1 - \frac{|\mathbf{r}_{ij}|}{\sigma_{ij}}\right)^2 \Theta\left(1 - \frac{|\mathbf{r}_{ij}|}{\sigma_{ij}}\right), \tag{2}$$

where ε is the energy scale, $\mathbf{r_{ij}}$ is the contact vector between particles i and j, σ_{ij} is the sum of the radii of particles i and j and Θ is the Heaviside step function. Thus, $U_{\text{tot}} = \sum_{ij} U(\mathbf{r}_{ij})$. From this potential, the forces between particles can be calculated as:

$$\mathbf{f}_{ij} = \frac{2\epsilon}{\sigma_{ij}} \left(1 - \frac{|\mathbf{r_{ij}}|}{\sigma_{ij}}\right) \Theta\left(1 - \frac{|\mathbf{r_{ij}}|}{\sigma_{ij}}\right) \hat{r}_{ij}. \tag{3}$$

We compute a nondimensionalized pressure using the microscopic formula [6, 15]

$$P \equiv -\frac{\bar{V_p}}{\varepsilon}\frac{\partial U_{\mathrm{tot}}}{\partial V} = \frac{\bar{V_p}}{\varepsilon V d}\sum_{i,j}\mathbf{f}_{ij}\cdot\mathbf{r}_{ij}, \tag{4}$$

where V is the volume of the system and $\bar{V_p}$ is the average particle volume.

For soft spheres the packing fraction φ can be increased, leading to new contacts and an increased pressure. We thus consider three natural quantities that measure distance from jamming:

- excess packing fraction, $\Delta\varphi = \varphi - \varphi_j$,
- excess contacts per particle δz, defined as $\delta z = (Z - Z_c)/N$ where Z is the number of contacts,
- pressure P.

Mean field theory predicts the following scaling relationships between these quantities [5]:

$$P = C_{p\varphi}\Delta\varphi \tag{5}$$

$$\delta z = C_{zp}P^{1/2} \tag{6}$$

with prefactors $C_{p\varphi}$ and C_{zp} which are functions only of dimension [6]. These and other scaling relationships have been thoroughly and repeatedly confirmed in low dimensional jamming, and are summarized concisely by the scaling theory of the jamming transition [1, 6–8, 16]. Moreover, mean field theory predictions of these prefactors can be derived as [5, 17]:

$$C_{p\varphi} = \frac{1}{d}\hat{C}_{p\varphi} \tag{7}$$

$$C_{zp} = d^{\frac{3}{2}}\sqrt{\frac{\log d}{\varphi_j}}\hat{C}_{zp} \tag{8}$$

where $\hat{C}_{p\varphi}$ and $\hat{C}_{zp}$ are finite constants in the $d \to \infty$ limit, which have not yet been explicitly calculated. Note that these relations are presented in a particular choice of units in the literature. We include details of the conversion to our dimensionless units in the supplement. *A priori*, it is not expected that these predictions will apply in low dimensions, in which the mean field assumption is not warranted. Even above upper critical dimensions, mean field theories often fail to accurately capture prefactors. As such, while these prefactors have been measured and reported, they have not received substantial attention [6, 18]. In this paper, we perform precision measurements of these prefactors in dimensions 2 to 10 and show that these mean field predictions are applicible even in low dimensions.

Computational Methods – We use pyCudaPacking [2], a GPU-based simulation engine, to generate energy minimized soft sphere packings. We do so for number of particles $N = 8192 - 32768$ and dimension $d = 2 - 10$. Our results suggest that $N = 8192$ is large enough to avoid finite size effects in $d < 10$, and for $d = 10$ we use a minimum system size of 32768. The particles are monodisperse, except in 2D in which we use equal numbers of bidisperse particles with a size ratio of 1:1.4 to prevent crystallization.

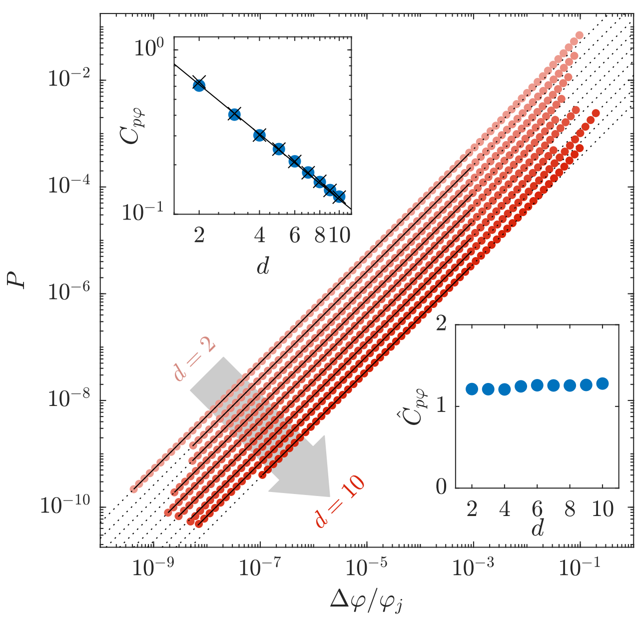

Figure 1: Measured pressure scales linearly with scaled excess packing fraction for systems from $d = 2$ to $d = 10$. Measured values for φ_j in our protocol are included in the supplemental material. Black lines show fits for $C_{p\varphi}$ using eqn 5. We exclude from the fit data with $\Delta\varphi/\varphi_j > 10^{-3}$, to avoid the effect of larger overlaps causing deviations from this power law. Dotted lines show the extension of fits beyond fitted range. Upper inset shows the measured values of $C_{p\varphi}$ (blue circles) to scale in agreement with the mean field prediction eqn 7, shown as a fit to a black line with $\hat{C}_{p\varphi} \approx 1.23$. Moreover, they are in precise agreement with predicted values from eqn 15 (black x's). Lower inset shows measured values of $\hat{C}_{p\varphi}$ calculated from the measured values of $C_{p\varphi}$ and eqn 7.

The packings are subject to periodic boundary conditions. We minimize the packings using the FIRE minimization algorithm [19] using quad precision floating point numbers in order to achieve resolution on the contact network near the jamming point.

Using the same methods as described in ref. [20], we start with randomly distributed initial positions, and apply a search algorithm to create systems approximately logarithmically spaced in $\Delta\varphi$. At each step we use the known power law relationship between energy and $\Delta\varphi$ to calculate an estimate of φ_j. We use this estimate to cal-

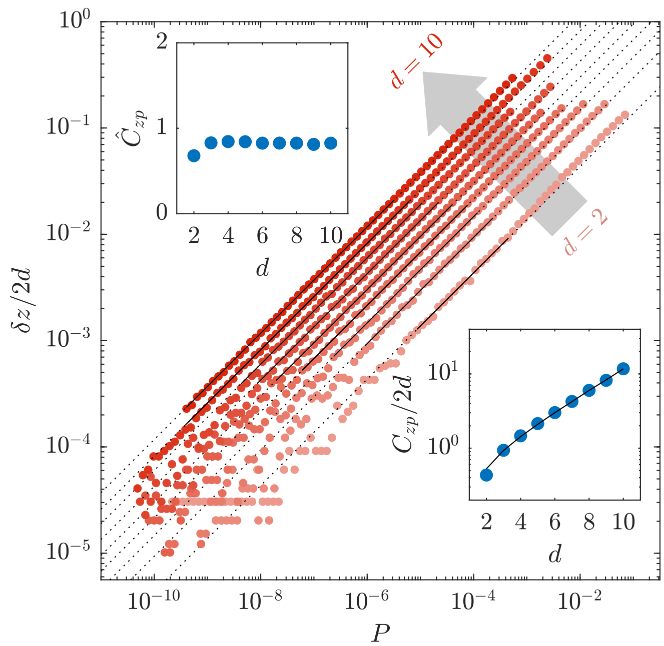

Figure 2: Measured excess contacts scales with the square root of pressure for systems from $d = 2$ to $d = 10$. Black lines show fits for C_{zp} using eqn 6. For our fits, we ignore high pressure data as in figure 1, and additionally exclude data with less than 40 excess contacts to avoid fitting to small number fluctuations. Dotted lines show the extension of our fits beyond fitted range. Lower inset shows the measured values of C_{zp} (blue circles), which scale in agreement with the mean field prediction eqn 8, shown as a fit to a black line using measured values of φ_j (included in supplement) and with $\hat{C}_{zp} \approx 0.82$. Upper inset shows measured values of $\hat{C}_{zp}$ calculated from the measured values of C_{zp} and eqn 8.

culate $\Delta\varphi$ and determine the next value of φ. We then adjust the packing fraction to this value of φ by uniformly scaling particle radii and minimizing the system.

Results – Figure 1 shows the measured linear scaling of pressure with packing fraction seperately for each dimension. For each dimension, we fit the data to eqn 5 to find $C_{p\varphi}$, considering only data close to jamming to avoid fitting to high pressure deviations from the scaling power law. The measured values of $C_{p\varphi}$ are shown in the inset to confirm the $\frac{1}{d}$ dimensional scaling predicted by mean field theory in eqn 7. A fit to this scaling provides a value of $\hat{C}_{p\varphi}$ of 1.23.

Figure 2 shows the measured square root scaling of excess contacts with pressure seperately for each dimension. For each dimension, we fit the data to eqn 6 to find C_{zp}, the values of which are shown in the inset. Beginning around 3 dimensions, the values of C_{zp} confirm the dimensional scaling predicted by mean field theory in eqn 8, and a fit to this scaling provides a value of $\hat{C}_{zp}$ of 0.82.

The values of both $C_{p\varphi}$ and C_{zp} are roughly consistent with values measured in previous studies [6, 18]. It has been recently suggested that the prestress, as defined in ref [21], is a better candidate to de-dimensionalize the relationship between pressure and excess contacts. However, we find that a substantially better collapse of our expected form of pressure than with prestress. For more details on prestress, see the attached supplement.

Discussion – The close agreement of our data with the mean field predictions in low dimensions suggests that the mean field assumption is not essential to derive these scaling and prefactor relations. In the spirit of discovering proofs for these relations free of the mean field assumption, we present here a derivation for the relation between pressure and excess packing fraction that does not rely on the mean field assumption, and additionally provides a prediction for $\hat{C}_{p\varphi}$.

Because P varies linearly with $\Delta\varphi$ near jamming, $C_{p\varphi}$ may be computed by calculating the bulk modulus near jamming:

$$C_{p\varphi} = \frac{\bar{V}_{\mathrm{p}} V}{\varphi\epsilon} \frac{\partial^2 U_{\mathrm{tot}}}{\partial V^2} = \frac{V}{N\epsilon} K, \tag{9}$$

where the derivative defining K is evaluated at $\Delta\varphi = 0$. We note that this approximation slightly overestimates $C_{p\varphi}$: the apparently linear average stress-strain curves of jammed packings are actually the average of many piecewise linear curves with discontinous drops in stress, thus the average slope is slightly less than the instantaneous slope [22].

At the unjamming point, the linear response of the system is that of a network of unstretched springs. Thus, at lowest order in pressure the bulk modulus is that of an unstressed spring network, which may be calculated in terms of the "states of self-stress", sets of possible spring tensions s which do not produce any net force on a particle [23–25]. Here we explain how to carry out this calculation for a monodisperse system in the unjamming limit; a correction for polydispersity is handled in the supplement.

We begin by defining the set of "affine bond extensions", a vector $\mathrm{E} \in \mathbb{R}^Z$ giving the amount by which each bond vector would increase under a unit volumetric expansion of the system. In linear elasticity, this simply induces an expansion of each length by $1/d$, so:

$$\mathrm{E}_\ell = \frac{1}{d} r_\ell, \tag{10}$$

where we emphasize that ℓ indexes the contacts in the system rather than the particles; r_ℓ is the distance between a particular pair of particles. In general we will use roman-text, unbolded letters to refer to vectors in this space $\mathbb{R}^Z$.

In the case that all springs have the same spring constant k (e.g. monodisperse packings), the bulk modulus may be written as the projection of these affine moduli onto the states of self stress [23–25]. At jamming, there is only one state of self stress, and so the bulk modulus may be computed exactly using the projection onto only this one state of self stress [24].

$$K = \frac{k}{V}\left(\sum_{\ell=1}^{Z} \mathrm{s}_{1,\ell}\mathrm{E}_\ell\right)^2 \tag{11}$$

What is the one special state of self stress that continues to exist all the way down to the jamming point? Since the packing is under positive pressure there exist forces f between all pairs of particles that are connected by contacts. For the packing to be in equillibrium, this set of contact forces must produce no net force on every particle, and thus by definition the vector f is always a state of self stress. Additionally the projection defined above requires states of self stress to be normalized, and so the state of self stress may be expressed as:

$$\mathrm{s}_{1,\ell} = \frac{1}{\sqrt{\mathrm{f}\cdot\mathrm{f}}}\mathrm{f}_\ell = \frac{1}{\sqrt{Z\langle f^2\rangle}}\mathrm{f}_\ell. \tag{12}$$

Furthermore at lowest order in P we have $\mathrm{r} = \sigma$, and we assume $Z \approx dN$. Thus, equation 11 reduces to

$$K = \frac{2Nk\sigma^2}{dV}\frac{\langle f\rangle^2}{\langle f^2\rangle} = \frac{2N\varepsilon}{dV}\frac{\langle f\rangle^2}{\langle f^2\rangle} \tag{13}$$

and thus via equation 9

$$C_{p\varphi} = \frac{2}{d}\frac{\langle f\rangle^2}{\langle f^2\rangle}, \tag{14}$$

for monodispersed spheres. The full calculation in the supplement shows that in the polydisperse case this becomes

$$C_{p\varphi} = \frac{2}{d}\frac{\langle \sigma f\rangle^2}{\langle \sigma^2 f^2\rangle}. \tag{15}$$

As long as the distribution of contact forces does not depend strongly on dimension, we thus predict the scaling of $C_{p\varphi}$ to agree with the asymptotic mean-field scaling. Because this proof does not invoke the mean field assumption, we expect this scaling to be correct in all dimensions. Moreover, we are able to calculate each value of $C_{p\varphi}$ by measuring the ratio of force distrubution moments. These values are calculated as in equation 15, and are shown in figure 1 to precisely predict the values of $C_{p\varphi}$.

Conclusion – The mean field theory of jamming predicts both the scaling exponents and the dimensional scaling of their prefactors. While the exponents have been previously verified, we have demonstrated that even some prefactors are well predicted in low dimensions by mean field theory. Although these prefactors should be considered especially sensitive to finite dimensional corrections, we find the mean field prediction to be exact in low dimensions. Is this a generic phenomenon, or are the quantities we have chosen to study in this work somehow specially unaffected by finite-dimensional correlations? Experience with critical phenomena suggests that they are both non-universal and challenging to compute, which has led to them being neglected. Our results demonstrate however that these prefactors may be computed exactly. These results call out for other theories which reproduce the mean-field results without such assumptions, or perhaps for a deeper understanding of why certain mean-field computations may be exact in finite dimensions.

Acknowledgments – We thank Francesco Zamponi for valuable discussion. This work benefited from access to the University of Oregon high performance computer, Talapas. This work was supported by National Science Foundation (NSF) Career Award DMR-1255370 and the Simons Foundation No. 454939.

[1] Andrea J. Liu and Sidney R. Nagel, "The Jamming Transition and the Marginally Jammed Solid," Annual Review of Condensed Matter Physics **1**, 347–369 (2010).
[2] Patrick Charbonneau, Eric I. Corwin, Giorgio Parisi, and Francesco Zamponi, "Universal Microstructure and Mechanical Stability of Jammed Packings," Physical Review Letters **109** (2012), 10.1103/PhysRevLett.109.205501.
[3] Patrick Charbonneau, Jorge Kurchan, Giorgio Parisi, Pierfrancesco Urbani, and Francesco Zamponi, "Glass and Jamming Transitions: From Exact Results to Finite-Dimensional Descriptions," Annual Review of Condensed Matter Physics **8**, 265–288 (2017).
[4] Giorgio Parisi and Francesco Zamponi, "Mean-field theory of hard sphere glasses and jamming," Reviews of Modern Physics **82**, 789–845 (2010).
[5] Giorgio Parisi, Pierfrancesco Urbani, and Francesco Zamponi, *Theory of Simple Glasses: Exact Solutions in Infinite Dimensions* (Cambridge University Press, New York, 2020).
[6] Corey S. OHern, Leonardo E. Silbert, Andrea J. Liu, and Sidney R. Nagel, "Jamming at zero temperature and zero applied stress: The epitome of disorder," Physical Review E **68** (2003), 10.1103/PhysRevE.68.011306.
[7] Corey S. O'Hern, Stephen A. Langer, Andrea J. Liu, and Sidney R. Nagel, "Random Packings of Frictionless Particles," Physical Review Letters **88** (2002), 10.1103/PhysRevLett.88.075507.
[8] Carl P. Goodrich, Andrea J. Liu, and James P. Sethna, "Scaling ansatz for the jamming transition," Proceedings of the National Academy of Sciences **113**, 9745–9750 (2016).
[9] Patrick Charbonneau, Eric I. Corwin, Giorgio Parisi, Alexis Poncet, and Francesco Zamponi, "Universal

Non-Debye Scaling in the Density of States of Amorphous Solids," Physical Review Letters **117** (2016), 10.1103/PhysRevLett.117.045503.

[10] Ludovic Berthier, Giulio Biroli, Patrick Charbonneau, Eric I. Corwin, Silvio Franz, and Francesco Zamponi, "Perspective: Gardner Physics in Amorphous Solids and Beyond," The Journal of Chemical Physics **151**, 010901 (2019), arXiv: 1902.10494.

[11] R.C. Dennis and E.I. Corwin, "Jamming Energy Landscape is Hierarchical and Ultrametric," Physical Review Letters **124** (2020), 10.1103/PhysRevLett.124.078002.

[12] Francesco Arceri and Eric I. Corwin, "Vibrational properties of hard and soft spheres are unified at jamming," arXiv:1912.05697 [cond-mat] (2019), arXiv: 1912.05697.

[13] Giorgio Parisi and Francesco Zamponi, "Amorphous packings of hard spheres for large space dimension," Journal of Statistical Mechanics: Theory and Experiment **2006**, P03017–P03017 (2006).

[14] M. Skoge, A. Donev, F. H. Stillinger, and S. Torquato, "Packing Hyperspheres in High-Dimensional Euclidean Spaces," Physical Review E **74**, 041127 (2006), arXiv: cond-mat/0608362.

[15] M. P. Allen, M. P. Allen, D. J. Tildesley, TILDESLEY ALLEN, and D. J. Tildesley, *Computer Simulation of Liquids* (Clarendon Press, 1989) google-Books-ID: O32VXB9e5P4C.

[16] Carl P. Goodrich, Andrea J. Liu, and Sidney R. Nagel, "Finite-Size Scaling at the Jamming Transition," Physical Review Letters **109** (2012), 10.1103/PhysRevLett.109.095704.

[17] Silvio Franz, Giorgio Parisi, Maxime Sevelev, Pierfrancesco Urbani, and Francesco Zamponi, "Universality of the SAT-UNSAT (jamming) threshold in non-convex continuous constraint satisfaction problems," SciPost Physics **2** (2017), 10.21468/SciPostPhys.2.3.019.

[18] James D. Sartor and Eric I. Corwin, "Direct measurement of force configurational entropy in jamming," Physical Review E **101** (2020), 10.1103/PhysRevE.101.050902.

[19] Erik Bitzek, Pekka Koskinen, Franz Ghler, Michael Moseler, and Peter Gumbsch, "Structural Relaxation Made Simple," Physical Review Letters **97** (2006), 10.1103/PhysRevLett.97.170201.

[20] Patrick Charbonneau, Eric I. Corwin, Giorgio Parisi, and Francesco Zamponi, "Jamming Criticality Revealed by Removing Localized Buckling Excitations," Physical Review Letters **114** (2015), 10.1103/PhysRevLett.114.125504.

[21] Masanari Shimada, Hideyuki Mizuno, Ludovic Berthier, and Atsushi Ikeda, "Low-frequency vibrations of jammed packings in large spatial dimensions," arXiv:1910.07238 [cond-mat] (2019), arXiv: 1910.07238.

[22] Meng Fan, Kai Zhang, Jan Schroers, Mark D. Shattuck, and Corey S. O'Hern, "Particle rearrangement and softening contributions to the nonlinear mechanical response of glasses," Physical Review E **96** (2017), 10.1103/PhysRevE.96.032602.

[23] S. Pellegrino, "Structural computations with the singular value decomposition of the equilibrium matrix," International Journal of Solids and Structures **30**, 3025–3035 (1993).

[24] M. Wyart, "On the rigidity of amorphous solids," Annales de Physique **30**, 1–96 (2005).

[25] T C Lubensky, C L Kane, Xiaoming Mao, A Souslov, and Kai Sun, "Phonons and elasticity in critically coordinated lattices," Reports on Progress in Physics **78**, 073901 (2015).

Supplemental Materials

Measured values of φ_j

In table I we show our measured values of φ_j which deviate somewhat at low dimensions from the mean field prediction in equation 1.

Table I: Measured values of φ_j in dimensions 2-10. These are fit to equation 1 to find a value of $\hat{C}_{\varphi} \approx 1.26$.

d	2	3	4	5	6	7	8	9	10
φ_j	0.85	0.65	0.46	0.31	0.20	0.13	0.078	0.049	0.029

MEAN FIELD PREDICTIONS OF PREFACTORS

Mean Field Prediction of Pressure vs Packing Fraction

Mean field theory predicts that pressure scales with packing fraction as follows [5]:

$$\hat{P} = \hat{C}_{p\varphi}(\hat{\varphi} - \hat{\varphi}_j) \tag{S1}$$

where $\hat{C}_{p\varphi}$ is a constant, and the hats over P and $\Delta\varphi$ signify that the quantities are scaled such to be fixed in the infinite dimensional limit, as follows:

$$\hat{P} = \frac{P^*}{\rho d} \tag{S2}$$

$$\hat{\varphi} = \frac{2^d}{d}\varphi \tag{S3}$$

where ρ is the number density, $\frac{N}{V}$, and P^* is the pressure which is calculated with assumed unit particle diameter. This relates to our pressure, P, as follows:

$$P = \frac{\varphi}{\rho}\frac{1}{d^2}P^*, \tag{S4}$$

where the factor of $\frac{\varphi}{\rho}$ unwraps their assumption of unit particle diameter, and the factor of $\frac{1}{d^2}$ comes from their potential, which explicitly contains a dimensional term:

$$U^*(r) = \frac{\epsilon d^2}{2}\left(\frac{r}{\ell} - 1\right)^2 \Theta\left(\ell - r\right). \tag{S5}$$

We can thus rewrite equation S2 in terms of our pressure P:

$$\hat{P} = \frac{d}{\varphi}P, \tag{S6}$$

and therefore equation S1:

$$\frac{d}{\varphi}P = \hat{C}_{p\varphi}\frac{2^d}{d}(\varphi - \varphi_j) \tag{S7}$$

$$P = \frac{\varphi}{d}\hat{C}_{p\varphi}\frac{2^d}{d}\Delta\varphi \tag{S8}$$

$$P = \frac{1}{d}\hat{C}_{p\varphi}\hat{\varphi}(\Delta\varphi). \tag{S9}$$

Noting that $\hat{\varphi}$ and $\hat{C}_{p\varphi}$ are constants in the infinite dimensional limit, mean field predicts a simple $1/d$ scaling of the prefactor between pressure and excess packing fraction.

Mean Field Prediction of Pressure vs Number Of Excess Contacts

The number of contacts, z, is predicted by mean field theory to have the form [5]:

$$\frac{z}{2d} = 1 + \hat{C}_{z\varphi}\sqrt{\hat{\varphi} - \hat{\varphi}_j} \tag{S10}$$

$$\frac{z}{2d} = 1 + \hat{C}_{z\varphi}\sqrt{\frac{2^d}{d}}\sqrt{\varphi - \varphi_j} \tag{S11}$$

for some constant $\hat{C}_{z\varphi}$.

The number of excess contacts, δz, therefore is predicted to scale as follows:

$$\frac{\delta z}{2d} = \hat{C}_{z\varphi}\sqrt{\frac{2^d}{d}}\sqrt{\varphi - \varphi_j} \tag{S12}$$

$$\delta z = 2d\hat{C}_{z\varphi}\sqrt{\frac{2^d}{d}}\sqrt{\varphi - \varphi_j}. \tag{S13}$$

We then rewrite this prediction in terms of the asymptotic form of φ_j in equation 1:

$$\delta z = 2d\hat{C}_{z\varphi}\sqrt{\frac{\hat{C}_\varphi \log d}{\varphi_j}}\sqrt{\varphi - \varphi_j}. \tag{S14}$$

Mean Field Prediction of Packing Fraction vs Number of Excess Contacts

By combining equations S9 and S14, we can also predict the relation between δz and P:

$$\delta z = 2d\hat{C}_{z\varphi}\sqrt{\frac{\hat{C}_\varphi \log d}{\varphi_j}}\sqrt{\frac{d}{\hat{C}_{p\varphi}}P} \tag{S15}$$

$$= 2d^{\frac{3}{2}}\hat{C}_{z\varphi}\sqrt{\frac{\hat{C}_\varphi}{\hat{C}_{p\varphi}}}\sqrt{\frac{\log d}{\varphi_j}}\sqrt{P} \tag{S16}$$

$$= \hat{C}_{zp}d^{\frac{3}{2}}\sqrt{\frac{\log d}{\varphi_j}}\sqrt{P} \tag{S17}$$

$$\tag{S18}$$

where we define $\hat{C}_{zp} = 2\hat{C}_{z\varphi}\sqrt{\frac{\hat{C}_\varphi}{\hat{C}_{p\varphi}}}$.

Excess Contacts vs Excess Packing Fraction Prefactor Scaling

From eqns 5 and 6 we can simply relate δz and φ as follows:

$$\delta z = C_{z\varphi}\left(\Delta\varphi\right)^{1/2} \tag{S19}$$

where clearly,

$$C_{z\varphi} = C_{zp}\sqrt{C_{p\varphi}}. \tag{S20}$$

In figure S1, we show this scaling seperately for each dimension. We fit each line to eqn S19 to find the values of the prefactor $C_{z\varphi}$ in each dimension, the values of which are shown in the inset. These values agree well with both the mean field prediction above $3D$, shown as a black line, and our calculated value from C_{zp} and $C_{p\varphi}$, shown as black x's in figures 2 and 1.

Accounting for polydispersity

To account for the case with varying spring constants we also form the matrix of inverse spring constants

$$k^{-1} = \frac{1}{2\varepsilon}\begin{pmatrix}\sigma_{ij}^2 & & \\ & \ddots & \\ & & \sigma_{kl}^2\end{pmatrix}. \tag{S21}$$

and the projection operator onto the states of self stress

$$S = \sum_{i=1}^{N\Delta z} |s_i\rangle \langle s_i| \,. \tag{S22}$$

In terms of these quantities, the bulk modulus may be written as [23–25]

$$\frac{\partial^2 E}{\partial V^2} = \frac{1}{V}\langle E| \, S \left(S\left(k^{-1}\right)S\right)^{-1} S \, |E\rangle \,. \tag{S23}$$

In the one SSS approximation, we can evaluate the two projected quantities that we need to evaluate equation S23. Equations 10 and 12 give

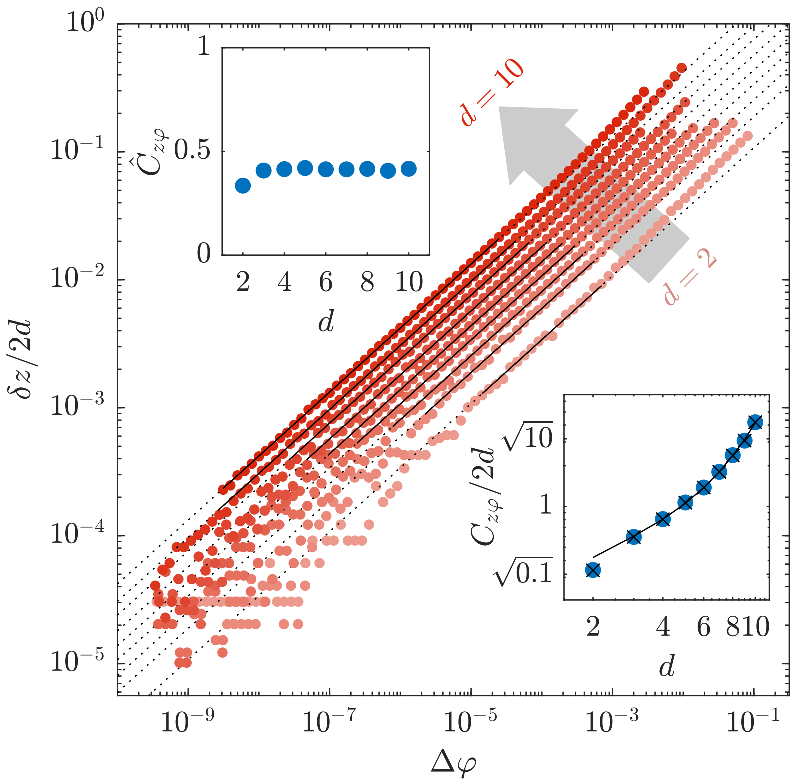

Figure S1: Measured excess contacts scales with the square root of excess packing fraction for systems from $d = 2$ to $d = 10$ (red circles). Black lines show the fits for C_{zp} using eqn S19. For our fits, we ignore data at high pressure and low contact number as in figure 2. Dotted lines show the extension of our fits beyond the fitted range. Inset shows the measured values of $C_{z\varphi}$ (blue circles), which scale in agreement with the mean field prediction eqn S14 using measured values of φ_j and $\hat{C}_\varphi$ (Table I), and with $\hat{C}_{z\varphi} \approx 0.41$. Additionally, to note consistency we show that our measured values of $C_{z\varphi}$ agree well with values calculated from our measurements of $C_{p\varphi}$ and C_{zp} using eqn S20 (black x's).

$$S|E\rangle = \langle s_0|f\rangle|s_0\rangle = \frac{\langle r|f\rangle}{d\sqrt{\langle f|f\rangle}}|s_0\rangle = \sqrt{Z}\frac{\langle rf\rangle}{d\sqrt{\langle f^2\rangle}}|s_0\rangle\,, \tag{S24}$$

and equations S21 and 12 give

$$Sk^{-1}S = |s_0\rangle\,\langle s_0|k^{-1}|s_0\rangle\,\langle s_0| = |s_0\rangle\frac{\langle\sigma^2 f^2\rangle}{2\epsilon\langle f^2\rangle}\langle s_0| \tag{S25}$$

$$\left(Sk^{-1}S\right)^{-1} = |s_0\rangle\frac{2\epsilon\langle f^2\rangle}{\langle\sigma^2 f^2\rangle}\langle s_0| \tag{S26}$$

Furthermore at lowest order in P we have $|r\rangle = |\sigma\rangle$, and we may assume $Z \approx dN$. Thus, equation S23 reduces to

$$K = \frac{2N\varepsilon}{dV}\frac{\langle\sigma f\rangle^2}{\langle\sigma^2 f^2\rangle}, \tag{S27}$$

and thus via equation 9

$$C_{p\varphi} = \frac{2}{d}\frac{\langle V_{\mathrm{particle}}\rangle\langle\sigma f\rangle^2}{\langle\sigma^2 f^2\rangle}. \tag{S28}$$

Prestress Comparison

It has recently been suggested the relationship between prestress and number of excess contacts collapses perfectly when compared across dimensions [21]. Prestress e is defined as in [21] as:

$$e = (d-1)\left\langle\frac{-V'(r_{ij})}{r_{ij}V''(r_{ij}}\right\rangle_{ij} \tag{S29}$$

and expected to scale as:

$$\delta z = C_{ez}e^{\frac{1}{2}} \tag{S30}$$

because it is proportional to pressure near the jamming transition. In figure S2, we examine the collapse of scaled excess contacts with prestress. In figure S2, we show that the collapse not quite perfect - there is a clear upward trend. This stands in contrast to the upper inset to figure 2, which shows $\hat{C}_{zp}$ to be nearly perfectly constant.

In fact, a short calculation shows that for this potential, our dimensionless pressure P as defined in equation 4 is related to the prestress by

$$P = 2\frac{\varphi_{\mathrm{J}}}{d-1}e. \tag{S31}$$

Thus, our better-fitting form for the $z-P$ relationship amounts to the statement that

$$\frac{\Delta z}{2d} = \hat{C}_{\varphi}\sqrt{\frac{d}{d-1}}\sqrt{e}. \tag{S32}$$

Thus our scaling forms agree with the statement of reference [21] in the infinite-d limit, although we see better fit with our form in low dimensions.

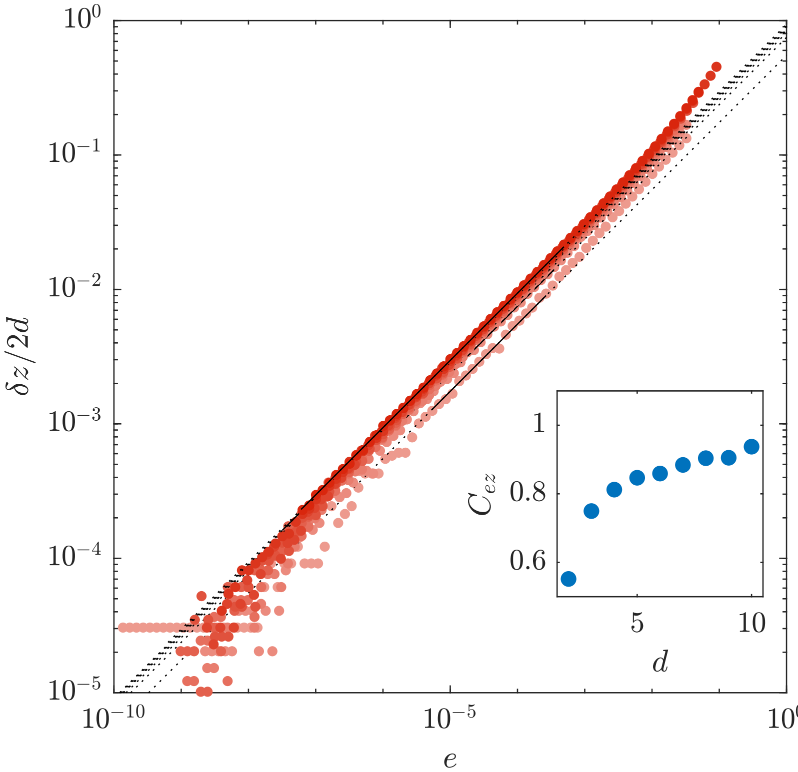

Figure S2: Scaled excess contacts scales with the square root of prestress for systems from $d = 2$ to $d = 10$ (red circles). Black lines show the fits for C_{ez} using eqn S30. The fits ignore high and low pressure data as in figure 2. Lower inset shows the measured values of C_{ez} which have a clear upward trend.